J Genet Resour2020;6(2): 185-194 *Homepage: http://sc.journals.umz.ac.ir/*

RESEARCH ARTICLE *DOI: 10.22080/jgr.2020.19334.1197*

J|G|R

Di-ethanolamine Might Cause Bone-related Complications Due to the Reduction of Osteogenic Differentiation and Induction of Oxidative Stress

Mohammad Hussein Abnosi and Setarehsadat Hosseini

Department of Biology, Faculty of Sciences, Arak University, Arak, Iran

ARTICLE INFO

Article history:
Received 12 April 2020
Accepted 18 June 2020
Available online 30 June 2020

Keywords:
BMSCs
Di-ethanolamine
Osteoblast mineralization
Osteoblasts differentiation
Oxidative stress
Viability

Corresponding authors:
✉ MH. Abnosi
m-abnosi@araku.ac.ir

p-ISSN 2423-4257
e-ISSN 2588-2589

ABSTRACT

Di-ethanolamine (DEA) is a well-known environmental pollutant used in manufacturing soap, detergent, body lotion, and other sanitary products. DEA has been reported to cause cytotoxicity in different tissue and cell, but no study was found to explain the toxic effect of DEA on rat bone marrow mesenchymal stem cells (BMSCs) differentiation. Thus in the present study, the differentiation property of BMSCs treated with DEA was investigated. BMSCs after 3rd passage cultured in osteogenic media in presence of 1 and 4 mM of DEA for 21 days. Then, the viability, based on 3-(4,5-dimethylthiazol-2-yl)-2,5-diphenyltetrazolium bromide or MTT) and morphology of nuclei and cytoplasm (using fluorescent dye), as well as osteoblasts mineralization property (based on quantitative alizarin red and calcium concentration), were studied. Also, sodium and potassium level, the activity of alanine transaminase, aspartate transaminase, alkaline phosphatase, and lactate dehydrogenase (LDH) were determined. The level of total-antioxidant capacity (TAC), malondialdehyde (MDA), and the activity of antioxidant enzymes (superoxide dismutase and catalase) also were estimated. The DEA treated cells showed nuclear enlargement and cytoplasm shrinkage as well as an increase in potassium level. Also based on LDH activity elevation, we observed a cellular anaerobic metabolism. Also, a significant increase in MDA was shown, while TAC and antioxidant enzyme activity was reduced. Finally, a significant decreased in cell viability and differentiation ability of BMSCs was observed. Since BMSCs are the cellular backup to generate osteoblasts, therefore its intoxication with DEA might cause bone complications, thus we recommend, prevention of DEA utilization in health-related products.

Please cite this paper as: Abnosi MH, Hosseini S. 2020. Di-ethanolamine might cause bone-related complications due to the reduction of osteogenic differentiation and induction of oxidative stress. *J Genet Resour* 6(2): 185-194. doi: 10.22080/jgr.2020.19334.1197.

Introduction

di-ethanolamine (DEA), a secondary amine-containing two molecules of ethanol is a very dangerous environmental pollutant (Libralato *et al*., 2010). The annual production of this compound was found to be 1.5 million tones (Frauenkron *et al*., 2012) and is used to manufacture soaps, detergents, washing machine powders, surfactants, cosmetics, shampoos, and pharmaceutical products (Bailey, 2007). Concerning its utilization, DEA contaminates water (Yordy and Alexander, 1981; Mathews *et al*., 1995), therefore, humans and animals are exposed to this environmental pollutant through the water and food chain. Different researches have shown that this chemical absorbs through the skin after 5-30 minutes when it is applied (Mathews *et al*. 1995; Kraeling *et al*., 2004). Also, it is well documented that, high concentration of DEA gets bio-accumulated in the liver, kidney, spleen, and brain (Mathews *et al*., 1997). Studies showed that the treatment of rats for 13 weeks with DEA contaminated water, caused microcytic anemia, kidney failure, brain, and spinal cord myelin sheath damage, seminiferous tubules destruction, liver damage, and skin inflammation (Melnick *et al*., 1994a; Melnick *et al*., 1994b). Also, previous studies revealed, that DEA caused a reduction of erythrocyte and reticulocyte number, a decrease

in hemoglobin and hematocrit level, and hemolysis of the RBCs (Melnick, 1992; Panchal *et al*., 2014). Niculescu *et al*. 2007), studied the effect of DEA (3 mM) on mouse neural precursor cells, they have concluded that this chemical-induced apoptosis and prevented cell proliferation due to intracellular choline reduction (Niculescu *et al*., 2007).

Bone marrow mesenchymal stem cells (BMSCs) as a cellular back up, can differentiate to osteoblasts and play an important role in bone repair and remodeling (Oliyai *et al*., 2017). Since there is intimate contact between bone marrow and peripheral blood, thus there is a chance of bone complications to happen. As DEA is hydrophilic, therefore it might get transferred via blood to bone marrow all over the skeletal system. To increasing the daily use of DEA in different industries, humans and animals are more exposed to its toxicity. Till now, we have found no data regarding the effect of DEA on BMSCs differentiation property in vitro and in vivo. Therefore, due to daily exposure to DEA and the importance of BMSCs in bone tissue repair and remodeling, this study was designed to investigate the mechanism of DEA effect on the differentiation property of BMSCs with correlation to the activity of metabolic enzymes and its anti-oxidative system.

Materials and Methods

Cell isolation and primary culture

The 6-8 weeks old male Wistar rats weighing 140 ± 20 g were purchased from Pasteur Institute (Tehran, Iran) and kept in the polyethylene cage at 27 ± 3 ^{o}C with convenient access to food and water. To separate the femora and tibia, based on the animal laboratory ethical committee role and regulation, the rats were anesthetized using chloroform (Merck, Germany). Then following the removal of surrounding connective tissues, the two ends of the bones were cut and the bone marrow was flushed out with the injection of 2 ml of Dulbecco's Modified Eagles Medium (DMEM, Gibco, Germany) supplemented with 15 % Fetal bovine serum (FBS, Gibco, Germany) and penicillin/ streptomycin (Gibco, Germany). The extracted bone marrow was centrifuged for 5 minutes at 2500 rpm and then re-suspended in fresh culture media. The extracted cell in culture media was plated in the culture flask and kept in an incubator at 37^{o}C with 5 % continuous injection of CO_2. The supernatant containing mostly red blood cells and non-adherent cells was decanted after 24 hours, then the fresh culture media was added and the flasks were returned to the incubator. The culture media was replaced every 3 days till 14 days when the bottom of the flasks was covered with a monolayer of the cell, the cells were detached from the flasks using trypsin-EDTA (Gibco, Germany) and washed with phosphate buffer saline (PBS). Then the washed cells were re-suspended in fresh culture media and plated in new flasks. To obtain 90-95 % purity of BMSCs (analyzed by flow cytometer, Germany, PARTEC Co.) two more passages were run by repeating the trypsinization method.

Osteogenic differentiation

The osteogenic differentiation of the cells was induced by culturing them in DMEM containing FBS (15 %), streptomycin/penicillin (1 %), 1mM sodium glycerophosphate, 50 µg/ml L-ascorbic acid, and 10^{-8} M dexamethasone (all the chemicals are from Sigma-Aldrich Company). The culture flasks were kept in an incubator at 37 ^{o}C with an atmosphere containing 5 % CO_2, and the culture medium was changed every 3 days until 21 days.

Cell exposure to DEA

The cells were cultured in an appropriate culture dish for 24 hours to make sure that the cells were attached to the bottom. Then the monolayer of the cells was treated with 1 and 4 mM of DEA (Merck, Germany) and incubated for 21days along with the control group which was treated only with culture media without any addition of DEA. The selected concentrations were chosen based on the dose-finding analysis (not shown) from a range of concentrations between 0.025 to 16 mM. Each sample was analyzed three times and reported as the mean value.

Cell viability assay

In a microplate the viability test was performed using MTT (4, 5dimethylthiazol-2-yl)-2,5-diphenyltetrazolium bromide) assay. In this analysis, the mitochondrial succinate dehydrogenase causes the conversion of yellow

tetrazolium into a violet crystal of formazan. To perform the analysis, 10 µl of tetrazolium solution [1 mg/ml of phosphate buffer saline (PBS)] was added to 100 µl of FBS free culture media and was kept for 4 hours in an incubator. Then after removing the culture media, 100 µl of dimethyl sulfoxide (DMSO) was added to each well and after 30 minutes the blue color solution was transferred to another well. The absorption of the solution was estimated using a microplate reader (SCO, diagnostic, Germany) at 505 nm (Abnosi and Masoomi, 2020).

Morphological observations

The cells were cultured for 21 days in the osteogenic media. Then to study the nuclear morphology, the cells were stained for 5 minutes in Hoechst 33342 solution (1 µg/ml of PBS) incubated in room temperature at dark. The stained cells were examined under an inverted fluorescence microscope (Olympus, IX70, Japan) equipped with a camera. Also, the cytoplasm morphology was studied using acridine orange (5 µg/ml in PBS). After staining, the cells were washed twice with PBS, examined, and photographed using an inverted fluorescence microscope (Olympus, IX70) equipped with a camera. The diameter of the nuclei and cytoplasm area of the cells was measured in µm and μm^2 respectively with the help of Motic Image software (Micro-optical group company version 1.2).

Quantification of matrix mineralization

Using PBS, the cells were washed and fixed with formaldehyde solution (10 % v/v) for 15 minutes, then 1 ml of alizarin red solution (ARS) (40 mM, pH 4.1) was added to each well of the plate and the plate was kept at room temperature for 20 minutes. Then 800 µl of acetic acid solution (10 % v/v) was added and the plate was continuously shaken for 30 minutes. Then the loosely attached cell was removed with the help of a cell scraper and transferred to a 1.5 ml tube. The tube was vortexed for 30 seconds and overlaid with 500 µl of mineral oil (Sigma-Aldrich) followed by heating it for 10 minutes at 85 ^{o}C.

The content of each tube was kept on ice for 5 minutes and centrifuged for 15 minutes at 16000 rpm. Then 500 µl of supernatant was transferred to a new tube and 200 µl of ammonium hydroxide (10 % v/v) was added to neutralize the solution. In a microplate, the absorption of 100 µl of the solution was determined at 405 nm using a microplate reader (SCO diagnostic, Germany). The absorption of the unknown was calculated using linear equation Y= 0.6899X+0.0921 with R2= 0.9882 derived from standard graph plotted by different concentration of alizarin red (the 40 mM solution of ARS was diluted 20 times with a 5:2 solution of acetic acid (10%) and ammonium hydroxide (10 %) to give a final concentration of 2 mM, then a series of 5 different dilutions was made from and the absorption was estimated at 405 nm). In the above equation, Y stands for absorbance and X stands for concentration (mM) of alizarin red solution (Abnosi and Masoomi, 2020).

Calcium concentration

After washing the monolayer of cells once with PBS and then with double distilled water (dH_2O), the cells were scraped from the bottom of the flask and collected in a 1.5 ml of the micro-centrifuge tube. After the determination of the cell weight, based on the equal weight; the calcium content of the cell was extracted using 50 µl of HCl (0.5 N) preserving them in cold for 24 hours. Using a commercial kit (Pars Azmoon, Iran), the concentration of total calcium was measured colorimetrically with the help of a spectrophotometer (Model $T80^{+}$ PG instrument manufacturing company, UK) at 630 nm after 5 minutes.

In this experiment, the calcium reacts with Arsenazo in neutral pH and a blue color develops where its intensity is proportional to the calcium concentration. A standard graph was plotted using various concentrations of $CaCl_2$, then the concentration of calcium in the samples was calculated using linear equation Y= 0.482X+0.0513 with R2= 0.997 where Y stands for absorption and X stands for concentration of calcium (mg/dl) (Abnosi and Masoomi, 2020).

Cell content extraction

Control and treated cells were kept in osteogenic media for 21 days, then the cells were washed with Tris-HCl (20mM Tris-HCl, pH 7.2) for two times. The cells were Scarp from the bottom of the flask and the content was extracted using

Tris-HCl. To break the cell membrane, the cell homogenate was kept at -20 °C overnight. Eventually, the homogenate was thawed and after making sure of complete membrane break down, it was centrifuged at 12000 g for 10 minutes. The total protein content was determined using the Lowry method (Lowry *et al*., 1951). *The* standard graph was plotted using bovine serum albumin and based on the linear equation Y=0.0008X+0.0357, with R2=0.998, the concentration of the samples was calculated. In the above equation, Y stands for absorbance and X stands for concentration of protein (µg). Further biochemical analysis was run based on the equal amount of protein in each sample.

ALT, AST, and LDH activity

The activity of lactate dehydrogenase (LDH), aspartate transaminase (AST), and alanine transaminase (ALT) was estimated using a commercial kit (Pars Azmoon, Iran), based on the equal amount of the protein. The analysis was carried out according to company instruction at 340 nm using a $T80^+$ spectrophotometer (Abnosi and Masoomi, 2019).

Alkaline phosphatase activity

The activity of alkaline phosphatase (ALP) was estimated using p-nitrophenyl phosphate (pNPP) as substrate according to company instruction (Pars Azmoon, Iran), based on the equal amount of the protein, at 410 nm with the help of a $T80^+$ spectrophotometer (Abnosi and Masoomi, 2019).

Sodium and potassium concentration

Using a flame photometer (Model PFP7, England), the total concentration of sodium and potassium in the extracted samples from the treated and control group of the cell was determined. In flame-photometry; the emission light of Na+ and K+ when burning is measured using different filters. The concentration of sodium (µg/ml) and potassium (µg/ml) was calculated by linear formula Y= 0.011X+ 0.0015with R2= 0.999 where Y= 0.084X+ 0.0058 with R2= 0.999 respectively when a standard graph was plotted using different concentration of NaCl and KCl. In the above equations, Y represents the absorption of emitted light and X represents the concentration of electrolyte (Abnosi and Masoomi, 2019).

Estimation of antioxidant enzymes activity

Superoxide dismutase activity

Using nitro-blue tetrazolium (NBT) (Sigma-Aldrich, N6876), the activity of superoxide dismutase (SOD) was estimated. 1 ml of the reaction mixture (6.1 mg NBT, 1.9 mg methionine, 7.9 mg riboflavin, and 3.3 mg EDTA was dissolved in potassium phosphate buffer with a final volume of 10 ml) was mixed with 50 µl of cell extract and kept for 10 minutes in a lightbox. A blank and control were also prepared in the same manner without the addition of the extracted sample. The blank tube was kept at dark and was used to adjust the $T80^+$ spectrophotometer at zero. The absorbance of each one of the samples was taken at 560 nm and the enzyme activity was reported as unit per minute for mg of protein required to cause 50 % inhibition (Abnosi and Babolghani, 2020).

Catalase activity

A reaction mixture containing 300 µl of H_2O_2 and 200 µl of potassium phosphate buffer (25 mM, pH 7.0) was prepared and its absorption was adjusted to 0.4 before the measurement was started. The activity of the catalase (CAT) enzyme was estimated based on the elimination of H_2O_2 for 2 minutes at 240 nm in presence of 50 µl of the sample using a $T80^+$ spectrophotometer. Taking 39.4 mM^{-1} cm^{-1} min^{-1} as the extinction coefficient the activity of CAT was calculated for one minute (Abnosi and Babolghani, 2020).

Determination of lipid peroxidation

Lipid peroxidation was determined based on the estimation of malondialdehyde (MDA) as an indicator. The measurement was carried out by mixing 1 ml of the reaction mixture (containing thiobarbituric acid (0.5 %) and trichloroacetic acid (20 %) in HCl) with 100 µl of the sample, kept in a boiling water bath for 30 minutes. The temperature of the mixture was reduced by holding it on ice for 15 minutes then centrifuging it for 15 minutes at 12000 rpm. The absorption was measured first at 523 nm and then at 600 nm using a $T80^+$ spectrophotometer. Then the values were subtracted from each other and using the extinction coefficient (1.55×10^3 μmol^{-1} cm^{-1}) the concentration of MDA was calculated and

reported as µM/ml (Abnosi and Babolghani, 2020).

Measurement of total antioxidant content

Total antioxidant content (TAC) of the samples were measured by mixing 1700 µl of the reaction solution (300 mM sodium acetate buffer (pH 6.3), 10 mM 2,4,6-Tris(2-pyridyl)-s-triazine (TPTZ) (Sigma-Aldrich, USA) dissolved in 40 mM hydrochloric acid (HCl) and 20mM Iron chloride), 850 µl distilled water and 150 µl of the sample. The mixture was kept at dark for 10 min and the absorbance was measured using a $T80^{+}$ spectrophotometer at 593 nm. Using the different concentrations of iron sulfate (FeSO4.7H2O) (Merck, Germany) a standard graph was plotted and TAC for each sample was calculated using linear formulas Y=0.0078X+0.02, R2=0.9923, where Y stands for absorption and X, stands for concentration (Abnosi and Babolghani, 2020).

Data analysis

SPSS (version 16, Sun Microsystems Inc., USA) was used to analyzed data. The analysis was carried out with the help of one-way analysis of variance (ANOVA) and Tukey honestly significant difference test as post hoc test. Results were presented as mean ± SD, and $P<0.05$ was considered as the minimum level of significance.

Results

Effect of DEA on cell viability and morphology

The MTT assay showed that the treatment of the cells with 1 and 4 mM of DEA for 21 days caused a significant ($p<0.05$) concentration-dependent reduction of viability compared to the control group. Viability reduction due to 4 mM was highly significant ($p<0.001$) with comparison to control and 1 mM groups (table 1).

Differentiated cells treated with 4 mM of DEA showed an increase in the diameter when compared to the control and 1 mM group (Figure 1). Also, the statistical analysis of the nuclei diameter confirmed the results of microscopic analysis, where a highly significant increase ($p<0.001$) in the nuclear diameter of the cells treated with 4 mM was estimated (Table 1).

On the other hand, the microscopic observation (Figure 2) and statistical analysis (Table 1) of the cell cytoplasm treated with different concentrations of DEA showed significant ($p<0.001$) reduction in the and shrinkage when compared to control one.

Table 1. Effect of DEA on cell viability (based on MTT) and morphology (based on nuclei diameter and cytoplasm area) of differentiated BMSCs after 21 days of treatment.

Conc. (mM)	Viability	Morphology	
	based on MTT	Nuclei diameter (µm)	Cytoplasm area ($µm^2$)
Control	0.53^{a}±0.02	10.99^{a} ± 0.71	448.65^{a} ± 10.05
1	0.34^{b}±0.03	10.19^{a} ± 0.39	284.13^{b} ± 13.10
4	0.13^{c}±0.01	21.25^{b} ± 0.40	301.80^{b} ± 2.90

Data are presented as means ± SD; in a column, means with different letter codes differ significantly from each other (ANOVA, Tukey test, $P < 0.05$).

Analysis of matrix mineralization:

After staining the differentiated cells with alizarin red, the matrix appeared in red. Macroscopic and microscopic observation revealed the reduction of alizarin red stain in the DEA treated groups (1 and 4 mM treated groups) (Figures 3). The statistical analysis of the data also showed a highly significant ($p<0.001$) reduction of matrix mineralization due to DEA treatment in both treated groups compared with the control (Table 2). Also, the analysis of calcium level extracted from differentiated cells treated with 1 and 4 mM of DEA confirmed the significant ($p<0.05$) reduction of calcium concentration as compared with the control group (Table 2), thus the above-mentioned results regarding the matrix formation was confirmed too.

Activity of enzymes

In the cell treated with 1 and 4 mM of DEA, the activity of lactate dehydrogenase (LDH), alanine transaminase (ALT), and aspartate transaminase (AST) increased significantly ($p<0.05$) compared to control one (Table 3). It is to be mentioned that the elevation of LDH was concentration-dependent and highly significant ($p<0.001$) too. We also observed a concentration-dependent and significant ($p<0.05$) increase in the activity of alkaline phosphatase (ALP) as compared with the control group. The ALP elevation in the

group treated with 4 mM of DEA was highly significant, with $p<0.001$ (Table 3).

Estimation of sodium and potassium concentration

The sodium level was not showing any changes in the treated groups as well as the control group (Table 4). Whereas, the potassium concentration in both the treated group (1 and 4 mM of DEA) showed a concentration-dependent significant reduction ($p<0.05$) when compared with the control group. It is to be mentioned that the reduction of potassium in the 4 mM treated group was highly significant ($p<0.001$) (Table 4).

Table 2. Effect of DEA on the matrix mineralization of differentiated cells, based on quantitative alizarin red (mM) staining and calcium (mg/dl) deposition in the matrix.

Concentration (mM)	Quantitative alizarin red	calcium concentration
Control	$0.256^{a}\pm0.026$	$30.91^{a}\pm0.88$
1	$0.136^{b}\pm0.009$	$26.96^{b}\pm0.37$
4	$0.119^{b}\pm0.006$	$25.18^{b}\pm0.50$

Data are presented as means ± SD; in a column, means with different letter codes differ significantly from each other (ANOVA, Tukey test, ($P < 0.05$).

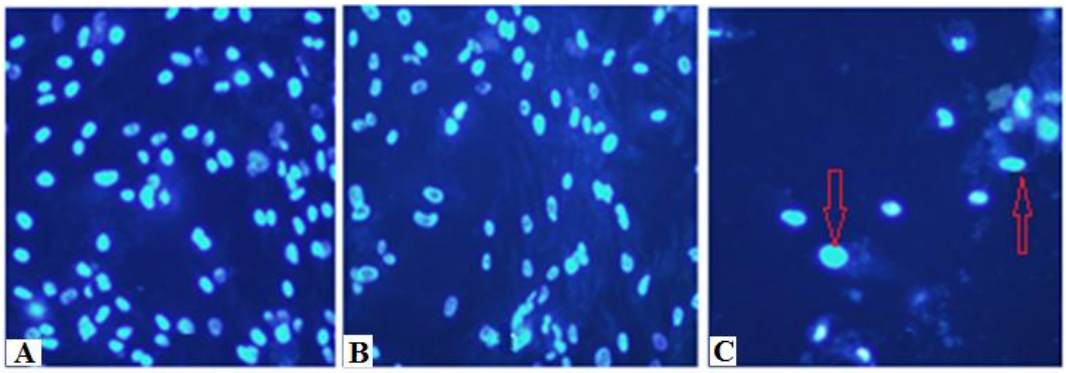

Fig. 1. Microscopic images of differentiated cells stained with Hoechst: A) control group; B) cells treated with 1 mM of DEA; C) cells treated with 4 mM of DEA; Arrows show nuclear enlargement in the 4 mM treated group (200 magnifications).

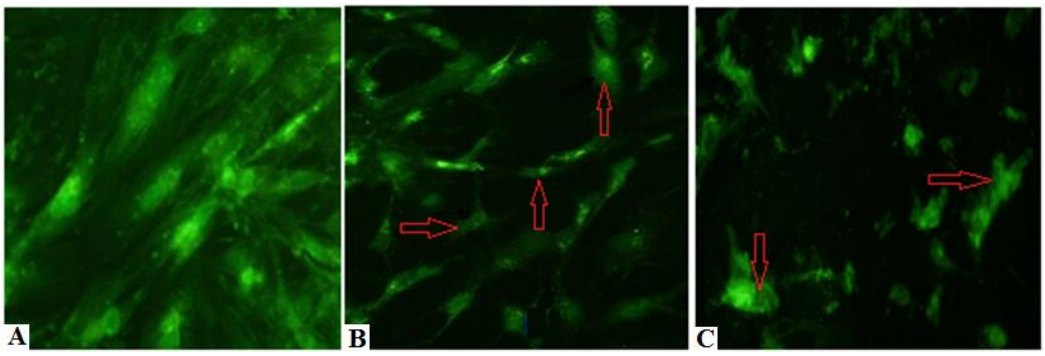

Fig. 2. Microscopic images of differentiated cells stained with acridine orange: A) control group; B) cells treated with 1 mM of DEA; C) cells treated with 4 mM of DEA; Arrows show a reduction in cytoplasm and aggregation of the cell body after treatment with 1 and 4 mM of DEA (200 magnifications).

Table 3. Effect of DEA on the activity (IU/L) of AST, ALT, LDH, and ALP of differentiated cells after 21 days of treatment.

Concentration (mM)	AST	ALT	LDH	ALP
Control	$217.52^{a}\pm13.60$	$20.18^{a}\pm0.33$	$902.97^{a}\pm10.74$	$414.06^{a}\pm37.30$
1	$295.70^{b}\pm18.18$	$22.27^{b}\pm0.76$	$1255.63^{b}\pm16.03$	$517.36^{b}\pm33.16$
4	$309.43^{c}\pm11.61$	$23.16^{c}\pm0.67$	$1358.92^{c}\pm37.93$	$619.49^{c}\pm34.49$

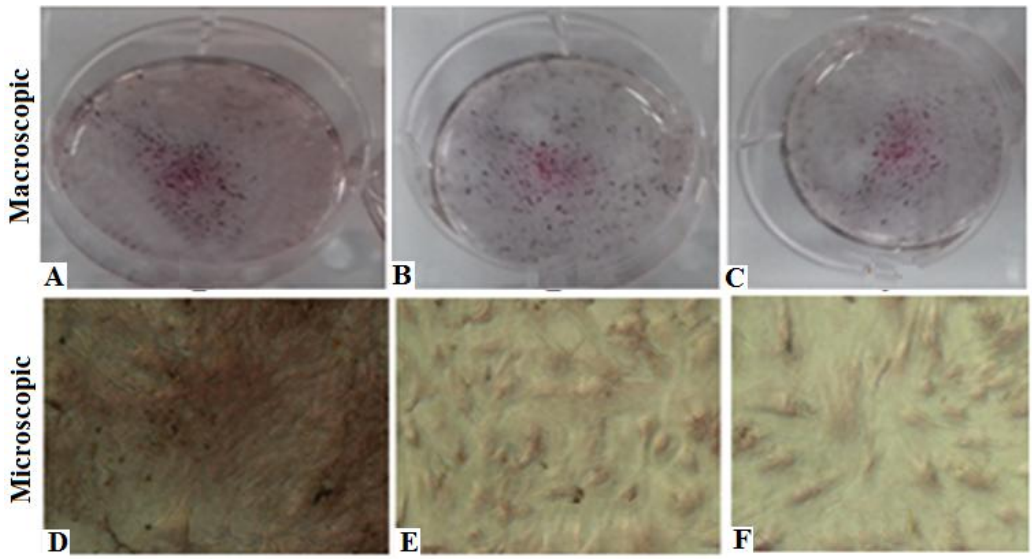

Fig. 3. Osteogenic confirmation of macroscopic and microscopic images: A and D) control group; B and E) cells treated with 1mM of DEA; C and F) cells treated with 4 mM of DEA.

Table 4. Effect of DEA on sodium and potassium levels of the differentiated cell after 21 days of treatment.

Conc. (mM)	Sodium (µg/dL)	Potassium (µg/dL)
Control	6.21^{a}±0.05	1.72^{a}±0.07
1	6.21^{a}±0.05	1.45^{b}±0.12
4	6.52^{a}±0.05	1.07^{c}±0.07

Data are presented as means ± SD; in a column, means with different letter codes differ significantly from each other (ANOVA, Tukey test, P < 0.05).

Oxidative stress determination

The statistical analysis of the data showed the total antioxidant capacity of the cells (TAC) and the activity of CAT as well as SOD reduced significantly ($p<0.05$) in the dedifferentiated cells treated with 1 and 4 mM of DEA. It should be mentioned that the 4 mM of DEA caused a highly significant ($p<0.001$) reduction in the activity of enzymes and TAC (Table 5). The level of malondialdehyde (MDA) increased significantly ($p<0.05$) in a concentration manner, while its elevation was highly significant ($p<0.001$) in the 4 mM treated group (Table 5) compared to control one.

Discussion

Several research groups have pointed the toxic effect of DEA on neural precursor cell, steroidogenesis, and red blood corpuscles (Niculescu *et al*., 2007; Panchal and Verma., 2016; Panchal *et al*., 2014). In the present study, the cell viability of differentiated BMSCs was decreased significantly due to DEA treatment in a concentration-dependent manner. During the differentiation process, many cellular and biochemical changes are happening, such as a morphological shift from long spindle to cuboidal and sphere in shape (Long *et al*., 2019), or metabolic activity down/upregulation (Shum *et al*., 2016) and organelle number increase/decrease (Zheng *et al*., 2020).

Table 5. The mean of total antioxidant capacity (TAC) (µg/mL) and malondialdehyde (MDA) (µM/mL) as well as activity of catalase (CAT) (Unit min-1 mg-1 protein) and superoxide dismutase (SOD) (Unit min-1 mg-1 protein) in the differentiated cells treated with DEA for 21 days.

Dose (mM)	MDA	CAT	SOD	TAC
Control	0.163^{a}±0.01	2.63^{a}±0.06	9.24^{a}±0.66	8.85^{a}±0.46
1	0.208^{b}±0.01	1.90^{b}±0.15	6.76^{b}±0.40	6.62^{b}±0.51
4	0.295^{c}±0.01	1.40^{c}±0.06	4.40^{c}±0.40	4.74^{c}±0.71

Data are presented as means ± SD; in a column, means with different letter codes differ significantly from each other (ANOVA, Tukey test, P < 0.05).

Although we found no supporting data, the treatment of the cells with DEA might have affected such mechanisms which ultimately resulted in the viability reduction of differentiated cells. The differentiated osteoblasts, following treatment with DEA for 21 days, showed an elevated level of LDH, ALT, and AST. These changes happen in the direction to change cell metabolism from aerobic to anaerobic (Ewing and Clegg, 1969). In the aerobic metabolism, the pyruvate which is generated during the glycolysis is converted to acetyl-CoA and enters the Krebs cycle which happens in mitochondria (Nelson and Cox, 2008). As it was observed in the MTT assay, due to DEA toxicity, the cell mitochondria were not functioning properly, thus the only remaining pathway to produce ATP in glycolysis. For glycolysis to continue the level of NAD^+ has to be maintained (Nelson and Cox, 2008), therefore the lactate dehydrogenase activity increases to generate NAD^+ via the production of lactic acid from pyruvate. Thus the increasing elevation of LDH activity happened to compensate for the poor energy level of the treated cells.

On the other hand, the activity of ALT and AST has increased in the same direction to use more pyruvate and facilitate the consumption of glucose by glycolysis. ALT is responsible to generate alanine from pyruvate in presence of glutamate (De Ritis *et al*., 1972) via transferring the amine group from glutamate to pyruvate. From the other side, also AST in presence of α-keto-glutarate would produce glutamate and oxaloacetate from aspartate (De Ritis *et al*., 1972). Thus in addition to the reformation of glutamate; the oxaloacetate, which has been formed, might be converted to pyruvate via phospho enol-pyruvate carboxykinase activity (Nelson and Cox, 2008). The above-mentioned reactions happen to assist the formation of ATP through anaerobic metabolism. In addition to metabolic imbalance, DEA caused the reduction of potassium levels. Although the potassium level was decreased, we observed no change in sodium concentration, which indicate that the change in potassium level happened independently form ATP dependent sodium/potassium pump (Clausen *et al*., 2017) while another pump such as a voltage-dependent potassium pump might be responsible for potassium increase in the differentiated cell.

In the differentiated osteoblasts, DEA induced oxidative stress, which was associated with an elevated level of MDA due to the reduction of SOD and CAT activity as well as TAC level (Ighodaro and Akinloye, 2018). Whenever the activity of antioxidant enzymes and non-enzymatic antioxidant level reduces, the ability of the cell to eliminate the free radicals also decreases, therefore the free radicals affect the membrane unsaturated fatty acids which initiate the program cell death (Ighodaro and Akinloye, 2018). We may also take into the consideration that the free radicals not only oxidize the membrane lipids but also oxidizes the proteins and nucleic acids which ultimately diminishes the cytoskeleton function (Gardiner *et al*., 2013), the activity of enzymes, and expression of the genes (Vrtačnik *et al*., 2018). Therefore, oxidative stress which is an important factor in the reduction of cell viability and differentiation ability might have been responsible to influence the function and structure of the biomolecule in the BMSCs.

DEA in a concentration-dependent manner reduced the differentiation ability of the BMSCs based on quantitative alizarin red analysis and matrix calcium concentration. Although the activity of ALP in the differentiated osteoblasts was significantly increased, the quantitative and qualitative alizarin red analysis showed that the matrix production significantly reduced following 21 days of treatment. Concerning the reduction of matrix biosynthesis, the elevation of ALP activity is un-expectable and more research has to be carried out to understand the mechanism. But based on our observations, malfunctioning of the calcium transporter (Blair *et al*., 2011) might have been a reason, since, in addition to phosphate, the presence of calcium is necessary for hydroxylapatite formation. Therefore, reduction of calcium despite enough phosphate might be the causative factor of low red color formation in alizarin red analysis; alizarin red dye selectively attaches to calcium.

In the present research, 1 and 4 mM of DEA caused a reduction of cytoplasm area, while the reduction of nuclei diameter was only observed in 4 mM concentration treatment. The reduction of the cytoplasm area could be due to the

induction of oxidative stress which causes membrane disruption and cytoplasm shrinkage. But an increase in nuclei diameter due to treatment with 4 mM of DEA is more difficult to be justified. Some studies on fibroblasts explain the nuclei enlargement based on cell senescence (Yoon *et al*., 2016). In another study, it was revealed that the cells neighbor to the malignant cell show enlargement in nuclei (Jevtić *et al*., 2014) which might be a sign of transformation, that has to be investigated in case of DEA toxicity. There are some proteins responsible for nuclei size, and it has been documented that, whenever the activity of these proteins has inhibited the size of the nuclei increases. Sirtuin and Nup188 are two of these proteins, which their reduction has been reported to be responsible for nuclei enlargement (Yoon *et al*., 2016; Jevtić *et al*., 2014). Therefore, the enlargement of nuclei in the treated cells might be due to the reduction of these proteins, involve in nuclei size, we recommend more research to be conducted on this matter.

Conclusion: DEA is used in a variety of sanitary products such as soap, shampoos, body lotion, and so on. According to our data, this chemical caused viability reduction, morphological changes, and osteogenic differentiation imbalance due to metabolic shift and induction of oxidative stress in BMSCs. As it was observed in BMSCs, this chemical might cause harm to other stem cells presented in body tissue where may result in serious public health problem. We recommend the authorities to prohibit the utilization of DEA in sanitary products, as well as its presence in drinking water, which has to be checked routinely.

References

Abnosi MH, Babolghani ZA. 2020. The inhibitory role of Di-2-ethylhexyl phthalate on osteogenic differentiation of mesenchymal stem cells via down-regulation of *RUNX2* and membrane function impairment. *Int J Med Toxicol Forensic Med* 10(2): 26673.

Abnosi MH, Masoomi S. 2020. p-Nonylphenol impairment of osteogenic differentiation of mesenchymal stem cells was found to be due to oxidative stress and down-regulation of *RUNX2* and *BMP*. *Endocr Metab Immune* 20: 1-11.

Abnosi MH, Masoomi S. 2019. Para-nonylphenol toxicity induces oxidative stress and arrests the cell cycle in mesenchymal stem cells of bone marrow. *Iran J Toxicol* 13: 1-8.

Bailey J. 2007. DEA in consumer products is safe. *FASEB J* 21: 296-297.

Blair HC, Robinson LJ, Huang CL, Sun L, Friedman PA, Schlesinger PH, Zaidi M. 2011. Calcium and bone disease. *Biofactors* 37: 159-167.

Clausen MV, Hilbers F, Poulsen H. 2017. The structure and function of the Na,K-ATPase isoforms in health and disease. *Front.Physiol* 8: 371.

Nelson DL, Cox MM. 2008. Glycolysis, gluconeogenesis, and the pentose phosphate pathway. *Lehninger principles of biochemistry* 4th Ed. New York: chapter 14. Pp 521-59.

De Ritis F, Coltorti M, Giusti G. 1972. Serum transaminase activities in liver disease. *Lancet* 1: 685-687.

Ewing RD, Clegg JS. 1969. Lactate dehydrogenase activity and anaerobic metabolism during embryonic development in *Artemia salina*. *Comp Biochem Physiol* 31: 297-307.

Frauenkron M, Melder JP, Ruider G, Rossbacher R, Höke H. 2012. Ethanolamines and propanolamines. Wiley-VCH Verlag GmbH & Co. KGaA, Weinheim. DOI: 10.1002/14356007.a10_001.

Gardiner J, Overall R, Marc J. 2013. The nervous system cytoskeleton under oxidative stress. *Diseases* 1: 36-50.

Ighodaro OM, Akinloye OA. 2018. First line defense antioxidants-superoxide dismutase (SOD), catalase (CAT) and glutathione peroxidase (GPX): their fundamental role in the entire antioxidant defence grid. *Alexandria Med J* 54: 287-293.

Jevtić P, Edens LJ, Vuković LD, Levy DL. 2014. Sizing and shaping the nucleus: mechanisms and significance. *Curr Opin Cell Biol* 28: 16-27.

Kraeling ME, Yourick JJ, Bronaugh RL. 2004. *In vitro* human skin penetration of diethanolamine. *Food Chem Toxicol* 42: 1553-1561.

Libralato G, Volpi Ghirardini A, Avezzù F. 2010. Seawater ecotoxicity of monoethanolamine, diethanolamine and triethanolamine. *J Hazard Mater* 176: 535-539.

Long EG, Buluk M, Gallagher MB, Schneider JM, Brown Justin L, 2019. Human mesenchymal stem cell morphology, migration, and differentiation on micro and nano-textured titanium. *Bioact Mater* 4: 249-255.

Lowry OH, Rosebrough NJ, Farr AL, Randall RJ, 1951. Protein measurement with the folin phenol reagent. *J Biol Chem* 193: 265-275.

Mathews JM, Garner CE, Black SL, Mathews HB. 1997. Diethanolamine absorption, metabolis, and disposition in rat and mouse following oral, intravenous and dermal administration. *Xenobiotica* 27: 733-746.

Mathews JM, Garner CE, Mathews HB. 1995. Metabolism, bioaccumulation, and incorporation of diethanolamine into phspholipids. *Chem Res Toxicol*. 8: 625-633.

Melnick RL, Mahler J, Bucher JR, Thompson M, Hejtmancik M, Ryan MJ, Mezza LE. 1994a. Toxicity of diethanolamine. 1. Drinking water and topical application exposure in F344 rats. *J Appl Toxicol* 14: 1-9.

Melnick RL, Mahler J, Bucher JR, Hejtmancik M, Singer A, Persing RL. 1994b. Toxicity of diethanolamine. 2. Drinking water and topical application exposures in B6C3F1 mice. *J Appl Toxicol* 14: 11-19.

Melnick R. 1992. NTP technical report on the toxicity studies of Diethanolamine (CAS No. 111-42-2) administered topically and in drinking water to F344/N Rats and B6C3F1 Mice. *Toxic Report Series* 20:1-10.

Niculescu MD, Renan W, Zhong G, Kerry AC, Steven HZ. 2007. Diethanolamine alters proliferation and choline metabolism in mouse neural precursor cells. *Toxicol Sci* 96: 321-326.

Oliyai M, Abnosi MH, Momeni HR. 2017. Myo-inositol at high concentration reduced viability and proliferation of rat bone marrow mesenchymal stem cells via electrolyte imbalance and elevation of aerobic metabolism. *J Genet Resour* 3: 18-25

Panchal S, Prajapati H, Verma RJ. 2014. Diethanolamine cytotoxicity on red blood corpuscles. *Int Res J Biological Sci* 3: 67-69.

Panchal S, Verma RJ. 2016. Effect of diethanolamine on testicular steroidogenesis and its amelioration by curcumin. *Asian Pascific J Reprod* 5: 128-131.

Shum LC, White NS, Mills BN, de Mesy Bentley KL, Eliseev RA. 2016. Energy metabolism in mesenchymal stem cells during osteogenic differentiation. *Stem Cells Dev* 25: 114-122.

Vrtačnik P, Zupan J, Mlakar V, Kranjc T, Marc J, Kern B, Ostanek B. 2018. Epigenetic enzymes influenced by oxidative stress and hypoxia mimetic in osteoblasts are differentially expressed in patients with osteoporosis and osteoarthritis. *Sci Rep* 8:1-2.

Yoon KB, Park KR, Kim SY, Han SY. 2016. Induction of nuclear enlargement and senescence by sirtuin inhibitors in glioblastoma cells. *Immune Netw* 16: 183-188.

Yordy JR, Alexander M. 1981. Formation of N-nitrosediethanolamine from diethanolamine in lake water and sewage. *J Environl Qual* 10: 266-270.

Zheng CX, Sui BD, Qiu XY, Hu CH, Jin Y. 2020. Mitochondrial regulation of stem cells in bone homeostasis. *Trends Mol Med* 1: 89-104.